

RESEARCH

Open Access



A novel model of autologous tooth transplantation for *the study of* nerve recruitment

Teresa E. Fowler¹, Doan T. Bloomquist², Caroline Glessner³, Poonam Patel³, Jeffrey N. James^{4,5}, Kathryn Bollinger^{1,2,6,7}, Lynnette P. McCluskey⁸ and Ryan F. Bloomquist^{3,9*}

Abstract

Background Limited treatment options exist for damaged nerves and despite impressive advances in tissue engineering, scientists and clinicians have yet to fully replicate nerve development and recruitment. Innervation is a critical feature for normal organ function. While most organs are innervated prior to birth, a rare example of postnatal nerve recruitment occurs in the natural development of secondary teeth during adolescence. Many animals undergo postnatal shedding of deciduous teeth with development and eruption of secondary teeth, a process requiring recruitment of nerve and vasculature to each tooth pulp for viability. Here, the investigators created a novel model for the study of postnatal innervation by exploiting the natural phenomenon of tooth-driven nerve recruitment.

Methods The investigators theorized that developing teeth possess a special capacity to induce innervation which could be harnessed in a clinical setting for nerve regeneration, and hypothesized that a transplant model could be created to capture this phenomenon. In this descriptive study, a rat model of autologous tooth transplantation and *de novo* nerve recruitment was developed by surgically transferring whole developing molars to the autologous tibia.

Results Downstream histological analysis performed 6 to 14 weeks after surgery demonstrated integration of molar into tibia in 81% of postoperative rats, with progressive pulpal expression of nerve marker β -tubulin III suggestive of neuronal recruitment.

Conclusions These findings provide a novel model for the study of organ transplantation and support the theory that developing dental tissues may retain nerve-inductive properties postnatally.

Keywords Dental regeneration, Neuron biology, Innervation, Molar, Tibia, Bioengineering

*Correspondence:

Ryan F. Bloomquist

ryan.bloomquist@uscmed.sc.edu

¹Department of Ophthalmology, Wellstar MCG Health, 1120 15th Street, Augusta, GA 30912, USA

²Department of Ophthalmology, Charlie Norwood Veterans Affairs Medical Center, 950 15th Street, Augusta, GA 30901, USA

³The Dental College of Georgia at Augusta University, 1430 John Wesley Gilbert Drive, Augusta, GA 30912, USA

⁴Present address: Department of Surgery, Wellstar MCG Health, 1120 15th Street, Augusta, GA 30912, USA

⁵Oral and Maxillofacial Surgery, Louisiana State University Health Sciences Center, 1100 Florida Ave, New Orleans, LA 70119, USA

⁶Department of Cellular Biology and Anatomy, Medical College of Georgia at Augusta University, 1460 Laney Walker Blvd, Augusta, GA 30912, USA

⁷The James and Jean Culver Vision Discovery Institute, Medical College of Georgia at Augusta University, 1120 15th Street, Augusta, GA 30912, USA

⁸Department of Neuroscience and Regenerative Medicine, Medical College of Georgia at Augusta University, 1462 Laney Walker Blvd, Augusta, GA 30912, USA

⁹University of South Carolina School of Medicine, 6311 Garners Ferry Road, Columbia, SC 29209, USA



© The Author(s) 2024. **Open Access** This article is licensed under a Creative Commons Attribution-NonCommercial-NoDerivatives 4.0 International License, which permits any non-commercial use, sharing, distribution and reproduction in any medium or format, as long as you give appropriate credit to the original author(s) and the source, provide a link to the Creative Commons licence, and indicate if you modified the licensed material. You do not have permission under this licence to share adapted material derived from this article or parts of it. The images or other third party material in this article are included in the article's Creative Commons licence, unless indicated otherwise in a credit line to the material. If material is not included in the article's Creative Commons licence and your intended use is not permitted by statutory regulation or exceeds the permitted use, you will need to obtain permission directly from the copyright holder. To view a copy of this licence, visit <http://creativecommons.org/licenses/by-nc-nd/4.0/>.

Background

Nerve deficits, both sensory and motor, can arise from trauma, disease, developmental abnormalities, or iatrogenically through surgery or in the instance of organ transplantation. As the bioengineering of organs becomes feasible, a need to recruit nerves to these tissues to allow function will arise. The critical problem in neuropathies is that, excluding rare phenomena, human neurons have limited replication potential when faced with an insult [1, 2]. A cadre of techniques including conduits, proteins, scaffolds, and transplanted stem cells have shown promise in repairing damaged nerves but are generally restricted to small, recent defects [3–6]. The ability to reliably replicate nerve recruitment in a laboratory setting is an increasing area of focus for scientists and clinicians alike because of the broad therapeutic implications in bioengineering for patients with nerve pathology.

De novo innervation of human tissues beyond embryogenesis is rare [7], with a notable exception found in the development of secondary teeth. In humans this process occurs once in childhood, but in other animals, such as fishes and reptiles, teeth with associated nerve branches are continuously replaced [8]. The tooth pulp contains nerves that are responsive to temperature and stimulation, as well as sympathetic fibers which modulate inflammation [9], vascular tone [10], and tissue homeostasis [11]. Innervation of newly formed teeth requires complex spatial and temporal coordination of neurotrophic factor expression by dental tissues [12]. For example, proteins of the nerve growth factor family are known to act as neurorecruiting signals in developing teeth and play a role in repair after injury [13, 14]. Brain-derived neurotrophic factor expression by dental papilla cells promotes neurite outgrowth and directional axon honing in vitro [15]. Glial cell-derived neurotrophic factor ligands enhance neuron survival and proliferation in the brain [16] and other tissues, and are highly expressed in developing teeth [17], promoting odontoblast differentiation [18], stem cell migration [19], and pulp proliferation after injury [20]. As we gain knowledge about neurotrophic factors in vitro and in vivo, a live animal model through which to study these complex interactions is needed.

Intriguingly, autotransplantation of teeth in a clinical setting has been used as an alternative to titanium implants for replacing damaged teeth. In adolescent humans with damaged 1st molars, unerupted 3rd molars transplanted to the 1st molar site have been shown to sense temperature at 1 year follow up [21], implying acquisition of secondary sensory innervation [22–25] with a functional connection of transplanted tooth nerve endings to permit central recognition of nociception. Specific donor tooth criteria have been proposed that must be met for the tooth to remain viable in autotransplantation, including the presence of open apical

foramina and immature roots [26–28]. Investigation into neurotrophic factors in rodent and human teeth has led to the proposal that dental tissues may be useful sources of signaling for treatment of damaged nerves [29].

With this information, the investigators theorized that a developing tooth retains neuro-inductive properties postnatally. The goal of this study was to establish a new model through which to uncover mechanisms of nerve recruitment for advancements in tissue engineering. The investigators hypothesized that a tooth could be transplanted to a distant site, which could be used as a model to study signals for the induction of nerve growth. The investigators tested this hypothesis by developing a novel autologous tooth transplantation to tibia technique in live rats and examining downstream histological features for evidence of nerve recruitment.

Methods

Animal selection and husbandry

Twenty-six female Sprague-Dawley rats aged 7–14 days were purchased (Envigo). All experiments involving live rats were approved by the Augusta University Institutional Animal Care and Use Committee (protocol #2012–0496) and performed in compliance with Animal Research: Reporting of In Vivo Experiments (ARRIVE) guidelines [30–32]. This number of rats was chosen in order to provide sufficient animals for sequential sacrifice and analysis, with replicates and controls, while minimizing animal usage where possible. Physical examination of each age-matched rat was performed to ensure appropriate size and weight; 2 animals were excluded due to small size.

Autologous transplantation surgical technique

All instruments were autoclaved and the field disinfected using 70% ethyl alcohol. The lead authors of this study were primary surgeons in all experiments for consistency. Rats were anesthetized with ketamine (30 mg/kg), xylazine (5 mg/kg), and acepromazine (1 mg/kg) (NexGen Pharmaceuticals) via peritoneal injection under the oversight of certified veterinary personnel in accordance with the Division of Laboratory Animal Services regulations at Augusta University. Toe pinch was performed to ensure adequate sedation. Ophthalmic ointment was applied for corneal protection, with a rodent pulse oximeter utilized for continuous intraoperative vital monitoring.

The left leg surgical site of each rat was shaved, and both the maxillary palate and proximal leg prepped with 10% betadine. An incision was made over the tibia with #15 blade scalpel, and overlying tissues were dissected to expose periosteum. A monocortical bony defect was drilled into the anterior tibia using a surgical handpiece (Stryker) and half-round latch-type dental bur (Henry Schein) with saline irrigation. The ipsilateral maxillary

third molar was extracted using a #11/12 dental explorer (Henry Schein) placed subgingivally and distal to the maxillary 2nd molar to engage the developing 3rd molar crown. Gentle pressure was applied in a distal occlusal direction to extract the tooth, taking care to avoid damage to the root apices and pulp. Hemostasis was achieved with compression. The tooth was immediately transferred to the tibial bony defect, where it was stabilized between the posterior and anterior bony cortices with the pulp in the tibial marrow. Overlying muscle and skin were sutured closed. 3 rats underwent tooth extraction and tibial preparation without transplantation as external controls, and all right tibias of transplant animals served as internal controls without manipulation.

At the conclusion of the operation, each rat was given a subcutaneous injection of carprofen (5 mg/kg) for pain control and enrofloxacin (10 mg/kg) (NexGen Pharmaceuticals) for infection prophylaxis. Rats recovered in empty cages under heat lamp and were monitored closely, turning every 15 min. They were observed daily until sacrifice for signs of pain or distress.

Sacrifice and tissue fixation

Sequential sacrifice was performed on a weekly basis from 6 to 14 weeks post-surgery. Rats were euthanized by carbon dioxide inhalation with secondary decapitation. Tibias were fixed in 10% neutral buffered formalin (NBF) for 48 h. Specimens were dissected and imaged with three-dimensional micro computed tomography (micro-CT) reconstruction (Skyscan 1174 scanner). Specimens were then rinsed with 100% water and decalcified for 2 weeks at 4 °C in solution containing 200 g ethylenediaminetetraacetic acid (EDTA), 950 mL water, and 50 mL of 10 normal sodium hydroxide adjusted to pH 7.4. EDTA solution was changed every 48 h. Next, specimens were dehydrated through a graded series of ethanol, mounted in paraffin, and sectioned in 5-micron slices.

Hematoxylin and eosin (H&E), immunohistochemistry (IHC)

H&E staining was performed using a tissue autoprocessor according to manufacturer instructions (Leica Biosystems). For IHC, slides were submerged in xylene twice for 10 min each for paraffin removal then immersed in 100% ethyl alcohol for two 10-minute periods. They were rehydrated through 75%, 50%, and 25% ethyl alcohol baths for 5 min each followed by 100% deionized water for two 10-minute periods. For antigen retrieval, slides were pressure-cooked in a water bath for 5 min at 110 °C. Sections were incubated for 30 min in blocking solution consisting of 3% vol/vol goat serum, 1% bovine serum, and 0.1% Triton-X 100 (ThermoFisher Scientific) followed by 24-hour incubation at 4 °C with 1:1000 mouse anti- β -tubulin III antibody (Sigma-Aldrich) in blocking solution. Slides were washed in PBS then incubated for 24 h at 4 °C

in 1:400 Alexa-Fluor 568 goat anti-mouse IgG (Molecular Probes) in blocking solution. Slides were again rinsed in PBS and stored in Vectashield mounting medium with DAPI (Vector Laboratories) until imaging with a confocal (Zeiss) or BX50 microscope (Olympus) equipped with epifluorescence and MetaMorph software (Molecular Devices).

Results

Autologous tooth transplantation

Rats were selected as a higher order model with defined dental roots and terminal teeth which continue development postnatally, like humans. Their large size and delayed tooth development relative to mice [33, 34] facilitated surgical manipulation. The tibia was selected as the recipient site due to its large size, ease of access, and nutrient-rich marrow space in which to insert the tooth. Of note, the choice of a tibial transplantation site distant from the jaw was made intentionally to investigate whether dental neuron recruiting capability was maintained with the tooth outside its native environment.

In humans, 3rd molars transplanted prior to root initiation failed due to pulpal prolapse, while those performed after complete closure of the apices developed pulpal necrosis [25, 26]. In keeping with these findings, a litter of 5 rats was sequentially sacrificed for 3rd molar staging and it was determined that at 26 days the root was underdeveloped, while at 32 days the apices were completely closed. Therefore, 28 days after birth was selected as the target age for surgery.

Surgical transplantation of 3rd molars to the autologous tibia was performed on eighteen 28-day old rats. 2 succumbed to intraoperative cardiopulmonary death, presumably from anesthesia rather than the procedure itself. Among 16 survivors, surgery was well-tolerated with no significant signs of stress or discomfort beyond the initial postoperative period, and there were no postoperative infections. Sequential sacrifice was performed weekly from 6 to 14 weeks post-surgery. After processing, 13 of 16 rats (81%) demonstrated integrated 3rd molars in their tibias. Teeth were not identifiable in the remaining 3 specimens. 3 sham control rats underwent tooth extraction and tibial preparation without transplantation and were sacrificed at 7, 10, and 14 weeks post-operatively, exhibiting no significant differences in recovery compared to transplant subjects.

At 28 days, 3rd molar roots measured 2–2.5 millimeters (mm), while the entire length of the tooth measured 3.5–4 mm with some variation measured intraoperatively using calipers. The target tooth corresponded to stage $R_{3/4}$ with a formed crown, root length $\frac{3}{4}$ of mature tooth, and open apices as described by Moorrees [35]. Figure 1 shows the intraoperative tibial defect before (1a) and after tooth insertion (1b), measuring 2.1 mm in

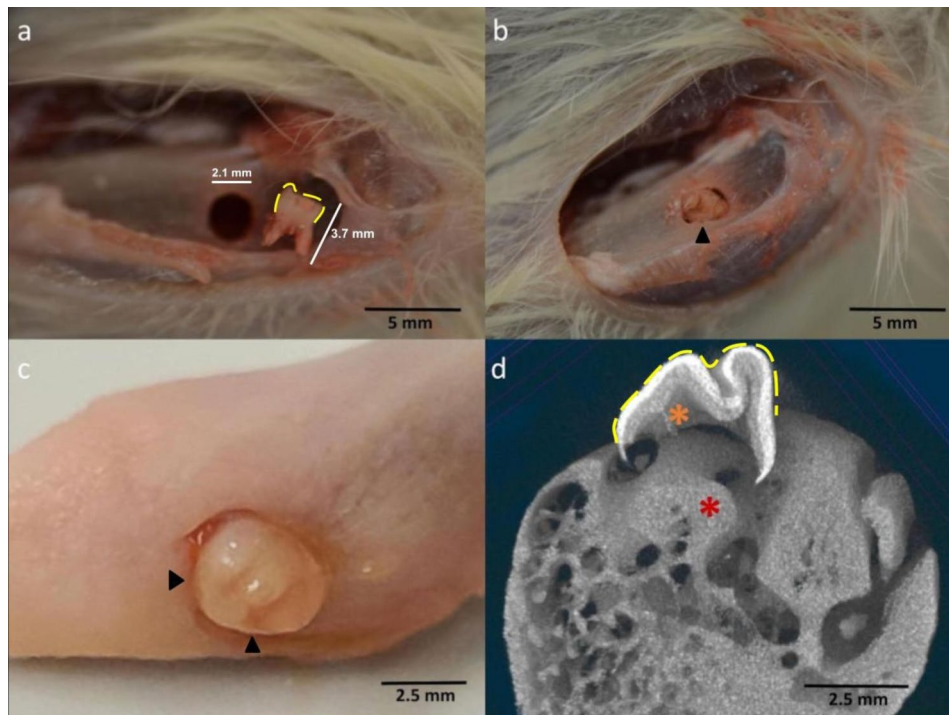


Fig. 1 Surgical technique and evidence of tooth integration. **(a)** Gross dissection of rat tibia showing an iatrogenic bony defect measuring 2.1 mm in diameter created with dental bur. To the right of the defect, the extracted third molar of the target 28-day stage is shown, with the crown outlined in yellow, measuring 3.7 mm in length. **(b)** Tibial defect after insertion of the extracted third molar, demonstrating the orientation of the tooth with pulp directed centrally and cusps extending outward towards skin (black arrowhead). **(c)** Transplanted third molar (arrowheads denoting crown) integrated into tibia after sacrifice, removal of soft tissue, and tissue fixation at 14 post-operative weeks. **(d)** Representative slice from a three-dimensional reconstruction of a transplanted tooth (cusps outlined in yellow) embedded in the tibia 7 weeks after surgery. The tooth is in the intended orientation, with the pulp (orange asterisk) contiguous with the central tibia (red asterisk)

diameter. The extracted third molar adjacent to the bony defect in Fig. 1a, with crown outlined in yellow, measured 3.7 mm in length. Figure 1c depicts an integrated molar with surrounding bony hypertrophy 14 weeks post-transplant, after soft tissue removal and fixation. Tooth cusps are visible extending from the bone, indicating that the intended orientation with pulp pointing towards the central tibia was maintained throughout recovery. Most of the integrated transplants exhibited apposition of tooth pulp to tibial marrow, though some migrated obliquely to varying degrees. Figure 1d is a reconstructed computed tomography image of an integrated transplant at 7 post-operative weeks, with enamel cusps superior and inferior soft tissue pulp continuous with tibial marrow. The root of the tooth is captured in this image and was noted to undergo resorptive remodeling after transplant. Sham controls sacrificed at 7 and 14-weeks post-transplant exhibited bony and periosteal wound healing in the area of tibial preparation (Supplemental Fig. 2).

Analysis 7-weeks post transplantation

The specimens in Fig. 2 were sacrificed 7 weeks post-transplant. Tooth structures in sagittal section were identifiable on H&E staining (Fig. 2a and b). Of note,

enamel is not visible due to decalcification required for sectioning (Fig. 2a). Adjacent to the enamel resides dentin, an avascular matrix of calcium hydroxyapatite and collagen deposited by odontoblasts [36] demonstrating characteristic weakly basophilic stain. Centrally, the pulp is highly cellular with neutrophilic infiltrate. Extensive bony remodeling was observed among these specimens. In Fig. 2a and b, eosinophilic hard tissue with morphological features similar to bone is seen between the dentin and tooth pulp, with an irregular margin suggestive of resorption by osteoclast-like cells at this interface. A layer of periosteum can be seen along the enamel surface as the tooth enters the tibia, eventually becoming continuous with the cellular tooth pulp.

IHC was performed using anti- β -tubulin III antibodies. In Fig. 2c and d, dental pulp can be seen with blue DAPI marking cell nuclei. Several discrete linear bundles of tubulin-expressing tissues traverse the cellular space between the tooth pulp and tibial marrow, present both in the cusp of the tooth pulp and adjacent to the tibial bony matrix. Of note, in specimens sacrificed at 6 weeks post-transplant we did not observe significant organized tubulin expression in the tooth pulp.

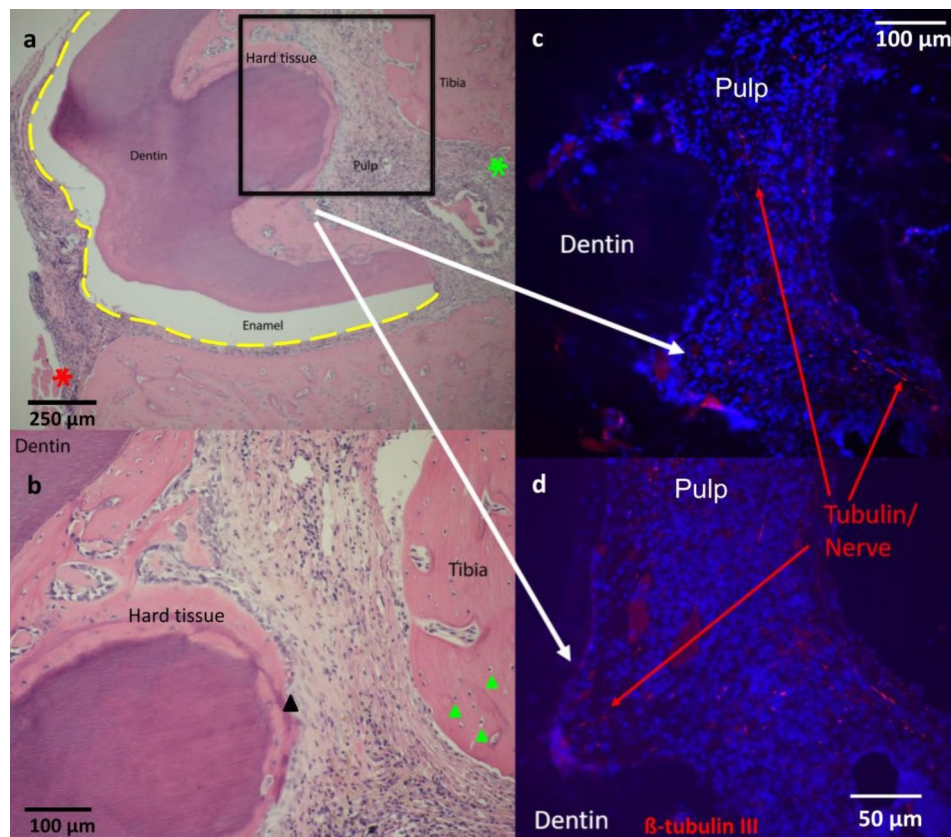


Fig. 2 H&E and IHC of teeth integrated into tibia at 7 post-operative weeks. These specimens were sacrificed 7 weeks post-operatively. On left, H&E staining in 5-micron sections of a transplanted tooth in sagittal plane integrated into the autologous tibia at 5X (a) and 10X (b). In 2a, the tooth layers are intact and labeled, with the crown outlined in yellow, the red asterisk drawing attention to reactive periosteum surrounding the integrated tooth, and the green asterisk denoting the interface between tibia and pulp. The area demarcated with the black box in 2a corresponds to the magnified area in 2b. In 2b, the black arrowhead denotes a layer of palisading cells at the interface between the hard tissue and tooth pulp, possibly of odontoblast origin. Green arrowheads indicate tibial osteocytes. IHC staining was for nerve marker β -tubulin III at 10X (c) and 20X (d), demonstrating a cellular tooth pulp with tubulin-expressing nerve fibers (red)

Analysis 14-weeks post transplantation

The subject in Fig. 3 was sacrificed 14 weeks after transplantation (Fig. 3). Inferiorly in Fig. 3a and magnified 3b, a molar encapsulated by proliferative fibrous tissue can be observed. In this representative specimen, the round body of the tooth can be seen in transverse plane with enamel surrounding dentin and pulp. A circular cusp of the tooth is visible centrally with associated layers. The highly cellular tooth pulp was similar in nuclear density to that of surrounding periosteum and soft tissues, but less than that of the highly cellular marrow of the corresponding tibia. Fibrosis was also noted in the pulp, with areas of low nuclear density across some specimens, suggesting a fibrotic scarring had occurred in some areas. In the superior aspect of the image, eosinophilic tibia with interspersed osteocytes surrounds a highly cellular basophilic medullary compartment. Irregular cement lines indicative of dysregulated remodeling were present in the cortical bone. Figure 3c and d show IHC from this same 14-week specimen at the level of the tooth root. Robust

tubulin expression is present in the tooth pulp as well as a band of staining peripherally, corresponding to the reactive fibrous capsule surrounding the transplant. Additionally, specimens sacrificed from 10 to 14 postoperative weeks demonstrated robust vascularization within the tooth pulp (Supplemental Fig. 1). Taken together, histology at 14 weeks post-transplant demonstrates tooth integration into tibia, cellular activity within the pulp, extensive bony remodeling, and the presence of tubulin-expressing cells within the tooth pulp.

Discussion

In this work, the investigators developed a rat model for autologous tooth transplantation to a distant site and demonstrated preliminary evidence of nerve recruitment. This supported the hypothesis that a model of tooth transplantation could be used to study the ability of developing teeth to induce innervation through nerve growth to a specific target. A monoclonal antibody to β -tubulin III, a tubulin isotype highly expressed in

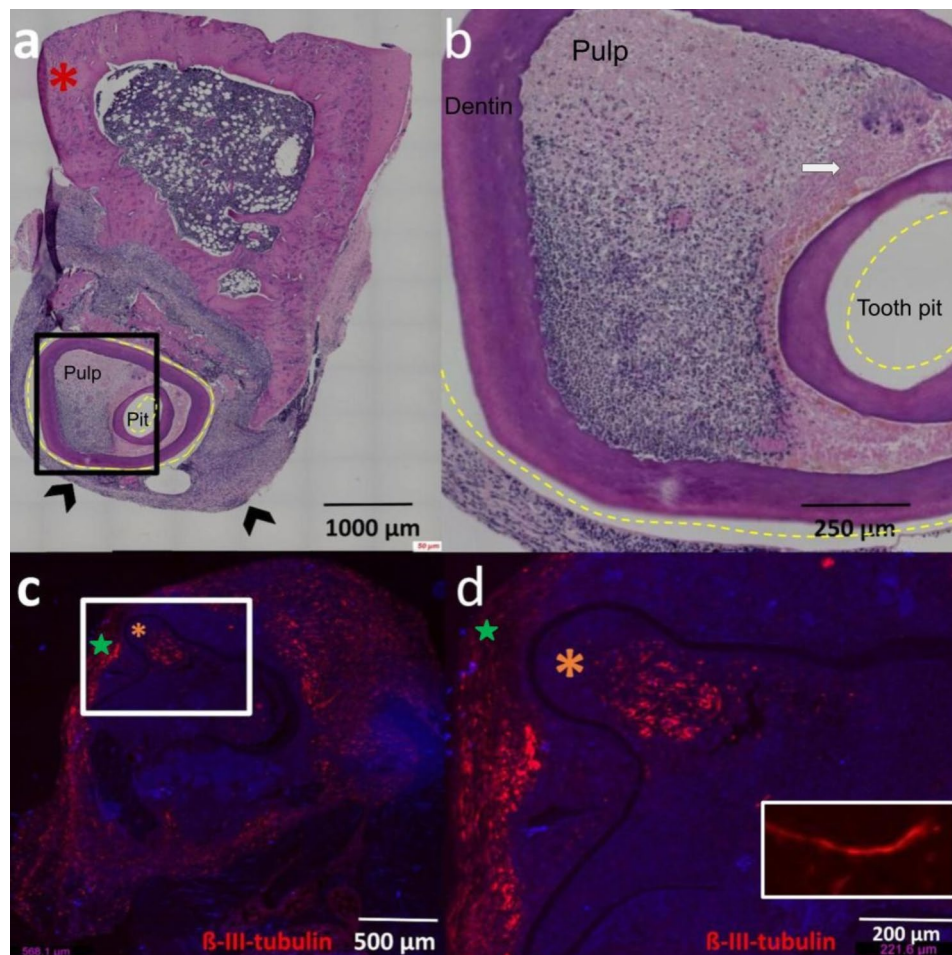


Fig. 3 H&E and IHC of integrated transplant tooth in tibia at 14 postoperative weeks. H&E at 5X (a) and 10X (b) in transverse section, with tooth enamel outlined in yellow in both images, and labeled pulp. In 3a, the red asterisk marks tibial cortex. A pit of the crown is captured in transverse plane and is labeled in 3a and 3b. We note the presence of a reactive periosteal capsule around the tooth (black arrowheads in 3a). The black square in 3a delineates the same area shown at higher magnification in 3b. In 3b, white arrow indicates fibrosis within tooth pulp. (c and d) IHC after sacrifice at 14 weeks post transplantation at 10X (c) and 20X (d) magnification. In 3c, the white square corresponds to the magnified image 3d. β -tubulin III stain is red, while cell nuclei are labeled blue with DAPI. Tubulin can be seen within the pulp chamber (orange asterisks), and within the periosteal layer (green stars). The magnified insert in 3d demonstrates a bundle of tubulin-positive cells

neurons [37–44] which has been shown to be important in neurite outgrowth [45, 46] and differentiation [47], was used as a marker of nerve tissue. This is a novel use of the rat model with many potential applications for further studies.

These results raise several interesting points of discussion. Rats were carefully staged prior to surgery, in keeping with the theory that nerve induction is temporally coordinated with a small window of potential. This insight was based on human clinical studies [27], in which autologously transplanted 3rd molars gain sensation only when surgery is performed at specific stages of development [26]. This brief time window of nerve recruitment may be helpful in uncovering specific neurogenic factors, and future studies include comparing the expression profiles of tissues capable of neuro-recruitment with pre- and post-cursors. The timing of sacrifice

was also noteworthy; organized bundles of tubulin expression were not present in specimens sacrificed at 6 weeks but were identifiable from 7 to 14 postoperative weeks (Figs. 2 and 3). This stain became increasingly robust as animals were given longer recovery periods. Since the tooth was completely separated from its native tissue during extraction, these tubulin-expressing cells presumably originated in the tibia and were stimulated by the immature molar to migrate. However, further lineage studies will be an important step required to be able to make strong conclusions about the origins of these cells.

Marked heterogeneity in the extent of bony hypertrophy, inflammation, and tooth resorption was observed between specimens. The recruitment of tubulin-expressing tissue despite this extensive remodeling and turnover supports the robust neurotrophic capacity of the developing molar. Intra-operatively, each tooth was carefully

oriented with pulp in the tibial marrow, though after sacrifice the integrated teeth had rotated to varying degrees during recovery. All successfully integrated transplants, however, maintained apposition of tooth pulp to tibial marrow, and it is likely that the 3 failed transplants were the result of extrusion from this nutrient-rich marrow. In this model, the marrow space provides a rich source of growth factors and cytokines [48] for tooth vitality, which may be similar to the platelet-rich plasma suggested to enhance healing in human tooth transplantation [21]. The hard tissue deposition between dentin and pulp (Fig. 2) affirms ample cellular activity and turnover within the transplant. It is possible that osteocytes and osteoclasts responsible for this deposition migrated from tibia, though the molecular stimulus for recruitment is unknown and requires further lineage tracing studies.

Autologous transplantation of 3rd molars to another site in the jaw has been previously described as a dental therapeutic, with clinical demonstration of vitality and bone integration [23, 25–27], but there is no proven clinical or animal model to study this at the molecular level. To our knowledge this is the first model of its kind, and this novelty is its greatest strength, lending to numerous potential future applications. Shortcomings of this study include small sample size, with the operation performed on only 18 rats, which limited the available downstream experiments that could be performed. However, as additional experiments are completed, characterization of the expression patterns of neuronal differentiation and growth factors can be performed at the mRNA and protein levels using additional markers, sequencing, and lineage tracing. Transcriptional analysis can be used to compare the expression profiles of teeth within the window of nerve recruitment potential to those past this time period, with the goal of identifying specific candidate factors responsible for nerve recruitment. In the short-term this model may aid in the discovery of dental borne tissues and molecular candidates that recruit nerves, as well as understanding changes occurring in the nerve cells themselves as neurites innervate teeth. In the long-term, this model may provide insight into therapeutic approaches for the induction of nerve growth to damaged and transplanted organs using dental-borne nerve recruitment signals.

Conclusions

The aim of this study was to develop an animal model through which to test whether developing teeth retain neuro-inductive properties postnatally, and whether tooth tissues can be used to induce nerve recruitment to a new site. Key findings include successful integration of transplants with ample pulpal cellular activity, including progressively robust expression of neuron marker β -tubulin III as recovery times were lengthened.

This work supports the hypothesis that developing teeth could be transplanted to a distant site in order to study the neuro-recruiting properties of teeth at specific stages and provides a model for further investigation into nerve recruitment mechanisms. This work provides a model to advance the knowledge gap regarding postnatal innervation and lays a foundation for future studies identifying specific neuroinductive molecules. Knowledge gained from this model could be used to aid in human regenerative therapeutics. The ability to regrow organs with predictable innervation has vast implications for transplantation, injury repair, degenerative disease, and developmental anomalies, with the potential to expand treatment options for patients suffering long term disabilities from nerve loss.

Abbreviations

ARRIVE	Animal Research: Reporting of In Vivo Experiments
EDTA	Ethylenediaminetetraacetic acid
H&E	Hematoxylin and eosin
IHC	Immunohistochemistry
Micro-CT	Micro computed tomography
Mm	Millimeters
NBF	Neutral buffered formalin

Supplementary Information

The online version contains supplementary material available at <https://doi.org/10.1186/s12903-024-04884-5>.

Supplemental Fig. 1: H&E and micro-CT demonstrating vascularization and tooth orientation. **(a)** H&E of a transplanted tooth embedded in tibia in sagittal section after 10 post-operative weeks. Within the pulp, vascularization can be seen with two arterioles labeled with red asterisks and one venule labeled with blue asterisks. **(b)** Magnified H&E view of integrated tooth pulp at 10 postoperative weeks, with vasculature labeled using black arrows. **(c)** Two-dimensional image of a three-dimensional micro-CT of 3rd molar (black arrowhead) integrated into tibia (white arrowhead) in a specimen sacrificed 7 weeks postoperatively

Supplemental Fig. 2: Control **(a)** Tibia from a sham control rat sacrificed 7 weeks after surgery after fixation and removal of soft tissue. **(b)** Micro-CT of tibia of control rat sacrificed 7 weeks postoperatively, with bony callous in the area of bony defect. **(c)** H&E of control rat tibia sacrificed 14 weeks postoperatively. Areas of bony remodeling can be seen (black arrowheads)

Author contributions

TEF contributed to data acquisition and analysis and drafted the manuscript. DTB contributed to data analysis and interpretation, drafted and critically revised the manuscript. CG contributed to data acquisition, critically revised the manuscript. PP contributed to data analysis, critically revised the manuscript. JNJ contributed to data interpretation, critically revised the manuscript. KB contributed to data interpretation, critically revised the manuscript. LPM contributed to data interpretation, critically revised the manuscript. RFB contributed to manuscript conception, design, data acquisition, analysis, and interpretation, critically revised the manuscript. All authors approved the final manuscript.

Funding

This work was funded by the Augusta University Career Development Scholars Program [grant number CDSP00002] and the National Institute on Deafness and Other Communication Disorders [grant number DC016668]. The funders played no role in study design, data collection, analysis, or the writing of this manuscript.

Data availability

No datasets were generated or analysed during the current study.

Declarations**Ethical approval**

Experiments involving live rats were approved by the Augusta University Institutional Animal Care and Use Committee (protocol #2012–0496) and performed in compliance with Animal Research: Reporting of In Vivo Experiments (ARRIVE) guidelines.

Consent for publication

Not applicable.

Competing interests

The authors declare no competing interests.

Received: 6 June 2024 / Accepted: 9 September 2024

Published online: 27 September 2024

References

- Moeendarbary E, Weber IP, Sheridan GK, Koser DE, Soleman S, Haenzi B, Bradbury EJ, Fawcett J, Franze K. The soft mechanical signature of glial scars in the central nervous system. *Nat Commun*. 2017;8(1):14787.
- Steward MM, Sridhar A, Meyer JS. Neural regeneration. In: *New perspectives in regeneration*. edn. Edited by Heber-Katz E, Stocum D: Springer; 2013: 163–191.
- Chalisserry EP, Nam SY, Park SH, Anil S. Therapeutic potential of dental stem cells. *J Tissue Eng*. 2017;8:1–17.
- Pfister LA, Papaloizos M, Merkle HP, Gander B. Nerve conduits and growth factor delivery in peripheral nerve repair. *J Peripher Nerv Syst*. 2007;12(2):65–82.
- Bellamkonda RV. Peripheral nerve regeneration: an opinion on channels, scaffolds and anisotropy. *Biomaterials*. 2006;27(19):3515–8.
- Siemionow M, Brzezicki G. Current techniques and concepts in peripheral nerve repair. *Int Rev Neurobiol*. 2009;87:141–72.
- Ashwell KW, Waite PM. Development of the peripheral nervous system. *Hum Nerv Syst* 2012:14–30.
- Richman JM, Handrigan GR. Reptilian tooth development. *Genesis*. 2011;49(4):247–60.
- Haug SR, Heyeraas KJ. Modulation of dental inflammation by the sympathetic nervous system. *J Dent Res*. 2006;85(6):488–95.
- Olgart L. Neural control of pulpal blood flow. *Crit Rev Oral Biol Med*. 1996;7(2):159–71.
- Haug SR, Brudvik P, Frstad I, Heyeraas KJ. Sympathectomy causes increased root resorption after orthodontic tooth movement in rats: immunohistochemical study. *Cell Tissue Res*. 2003;313(2):167–75.
- Jernvall J, Thesleff I. Tooth shape formation and tooth renewal: evolving with the same signals. *Development*. 2012;139(19):3487–97.
- Byun JH, Lee JH, Choi YJ, Kim JR, Park BW. Co-expression of nerve growth factor and p75NGFR in the inferior alveolar nerve after mandibular distraction osteogenesis. *Int J Oral Maxillofac Surg*. 2008;37(5):467–72.
- Mahdee A, Eastham J, Whitworth J, Gillespie J. Evidence for changing nerve growth factor signalling mechanisms during development, maturation and ageing in the rat molar pulp. *Int Endod J*. 2019;52(2):211–22.
- De Almeida JFA, Chen P, Henry MA, Diogenes A. Stem cells of the apical papilla regulate trigeminal neurite outgrowth and targeting through a BDNF-dependent mechanism. *Tissue Eng Part A*. 2014;20(23–24):3089–100.
- Granhölm AC, Reyland M, Albeck D, Sanders L, Gerhardt G, Hoernig G, Shen L, Westphal H, Hoffer B. Glial cell line-derived neurotrophic factor is essential for postnatal survival of midbrain dopamine neurons. *J Neurosci*. 2000;20(9):3182–90.
- Luukko K, Suvanto P, Saarna M, Thesleff I. Expression of GDNF and its receptors in developing tooth is developmentally regulated and suggests multiple roles in innervation and organogenesis. *Dev Dyn*. 1997;210(4):463–71.
- De Vicente JC, Cabo R, Ciriaco E, Laura R, Naves FJ, Silos-Santiago I, Vega JA. Impaired dental cytodifferentiation in glial cell-line derived growth factor (GDNF) deficient mice. *Ann Anat*. 2002;184(1):85–92.
- Xiao N, Yu WY, Liu D. Glial cell-derived neurotrophic factor promotes dental pulp stem cell migration. *J Tissue Eng Regen Med*. 2018;12(3):705–14.
- Woodnutt D, Wager-Miller J, O'Neill P, Bothwell M, Byers M. Neurotrophin receptors and nerve growth factor are differentially expressed in adjacent nonneuronal cells of normal and injured tooth pulp. *Cell Tissue Res*. 2000;299(2):225–36.
- Gonzalez-Ocasio J, Stevens M. Autotransplantation of third molars with platelet-rich plasma for immediate replacement of extracted non-restorable teeth: a case series. *J Oral Maxillofac Surg* 2017, 75(9):1833.e1831–1833.e1836.
- Ahlberg K, Bystedt H, Eliasson S, Odenrick L. Long-term evaluation of auto-transplanted maxillary canines with completed root formation. *Acta Odontol Scand*. 1983;41(1):23–31.
- Bae JH, Choi YH, Cho BH, Kim YK, Kim SG. Autotransplantation of teeth with complete root formation: a case series. *J Endod*. 2010;36(8):1422–6.
- Akiyama Y, Fukuda H, Hashimoto K. A clinical and radiographic study of 25 autotransplanted third molars. *J Oral Rehabil*. 1998;25(8):640–4.
- Andreasen J, Paulsen H, Yu Z, Ahlquist R, Bayer T, Schwartz O. A long-term study of 370 autotransplanted premolars. Part I. Surgical procedures and standardized techniques for monitoring healing. *Eur J Orthod*. 1990;12(1):3–13.
- Tsukiboshi M. Autotransplantation of teeth: requirements for predictable success. *Dent Traumatol*. 2002;18(4):157–80.
- Rohof EC, Kerdiq W, Jansma J, Livas C, Ren Y. Autotransplantation of teeth with incomplete root formation: a systematic review and meta-analysis. *Clin Oral Investig*. 2018;22:1613–24.
- Kristerson L. Autotransplantation of human premolars: a clinical and radiographic study of 100 teeth. *Int J Oral Surg*. 1985;14(2):200–13.
- Nosrat I, Seiger Å, Olson L, Nosrat CA. Expression patterns of neurotrophic factor mRNAs in developing human teeth. *Cell Tissue Res*. 2002;310(2):177–87.
- Percie du Sert N, Hurst V, Ahluwalia A, Alam S, Avey MT, Baker M, Browne WJ, Clark A, Cuthill IC, Dirnagl U. The ARRIVE guidelines 2.0: updated guidelines for reporting animal research. *J Cereb Blood Flow Metab*. 2020;40(9):1769–77.
- Kilkenny C, Browne W, Cuthill IC, Emerson M, Altman DG. Animal research: reporting in vivo experiments: the ARRIVE guidelines. *Br J Pharmacol*. 2010;160(7):1577.
- Kilkenny C, Browne WJ, Cuthill IC, Emerson M, Altman DG. Improving bioscience research reporting: the ARRIVE guidelines for reporting animal research. *PLoS Biol*. 2010;8(6):e1000412.
- Cai J, Cho S-W, Kim J-Y, Lee M-J, Cha Y-G, Jung H-S. Patterning the size and number of tooth and its cusps. *Dev Biol*. 2007;304(2):499–507.
- Ko D, Kelly T, Thompson L, Uppal JK, Rostampour N, Webb MA, Zhu N, Belev G, Mondal P, Cooper DM. Timing of mouse molar formation is independent of jaw length including retromolar space. *J Dev Biol*. 2021;9(1):8.
- Moorrees CF, Fanning EA, Hunt EE Jr. Age variation of formation stages for ten permanent teeth. *J Dent Res*. 1963;42(6):1490–502.
- Goldberg M, Kulkarni AB, Young M, Boskey A. Dentin: structure, composition and mineralization. *Front Biosci*. 2011;3:711.
- Lee MK, Tuttle JB, Rebhun LI, Cleveland DW, Frankfurter A. The expression and posttranslational modification of a neuron-specific β -tubulin isotype during chick embryogenesis. *Cell Motil Cytoskel*. 1990;17(2):118–32.
- Roskams A, Cai X, Ronnett G. Expression of neuron-specific beta-III tubulin during olfactory neurogenesis in the embryonic and adult rat. *Neurosci*. 1998;83(1):191–200.
- Draberova E, Lukás Z, Ivanyi D, Víklícký V, Dráber P. Expression of class III β -tubulin in normal and neoplastic human tissues. *Histochem Cell Biol*. 1998;109:231–9.
- Wang Z, Sugano E, Isago H, Hiroi T, Tamai M, Tomita H. Differentiation of neuronal cells from NIH/3T3 fibroblasts under defined conditions. *Dev Growth Differ*. 2011;53(3):357–65.
- LeClair EE, Topczewski J. Development and regeneration of the zebrafish maxillary barbel: a novel study system for vertebrate tissue growth and repair. *PLoS ONE*. 2010;5(1):e8737.
- Menezes J, Luskin MB. Expression of neuron-specific tubulin defines a novel population in the proliferative layers of the developing telencephalon. *J Neurosci*. 1994;14(9):5399–416.
- Abrous DN, Koehl M, Le Moal M. Adult neurogenesis: from precursors to network and physiology. *Physiol Rev*. 2005;85(2):523–69.
- Katsetos CD, Herman MM, Mörk SJ. Class III β -tubulin in human development and cancer. *Cell Motil Cytoskeleton*. 2003;55(2):77–96.
- Kapitein LC, Hoogenraad CC. Building the neuronal microtubule cytoskeleton. *Neuron*. 2015;87(3):492–506.

46. Qu C, Dwyer T, Shao Q, Yang T, Huang H, Liu G. Direct binding of TUBB3 with DCC couples netrin-1 signaling to intracellular microtubule dynamics in axon outgrowth and guidance. *J Cell Sci.* 2013;126(14):3070–81.
47. Cao S, Du J, Lv Y, Lin H, Mao Z, Xu M, Liu M, Liu Y. PAX3 inhibits β -Tubulin-III expression and neuronal differentiation of neural stem cell. *Biochem Biophys Res Commun.* 2017;485(2):307–11.
48. Soltan M, Smiler D, Choi JH. Bone marrow: orchestrated cells, cytokines, and growth factors for bone regeneration. *Implant Dent.* 2009;18(2):132–41.

Publisher's note

Springer Nature remains neutral with regard to jurisdictional claims in published maps and institutional affiliations.